Remarkable suppression of the $e^+e^- \to \pi^+\pi^-$ contribution error into muon $g-2$

E. Bartoš[a], S. Dubnička[a], A.-Z. Dubničková[b] and A. Liptaj[a]

[a]Inst. Phys., Slovak Acad. Sci., Dúbravská cesta 9, 845 11 Bratislava, Slovak Republic

[b]FMPI Comenius University, Mlynská dolina, 842 48 Bratislava, Slovak Republic

We use the unitary and analytic model of the pion electromagnetic form factor in order to evaluate in the lowest order the $e^+e^- \to \pi^+\pi^-$ contribution into the muon magnetic anomaly. We demonstrate, that this technique enables us to reduce the uncertainty of the theoretical prediction importantly in comparison to usual approaches, where the measured data are integrated directly.

1. Introduction and Motivation

The question of an experimental evidence of physics beyond the Standard Model (SM) has been and still is an issue in particle physics. This topic is especially popular nowadays, when new high-energy experiments are being constructed and put in work. Regarding the SM as a low-energy approximation of a more general theory, one can expect the new physics to manifest itself in two ways: important effects in measurements at high energies or small effects at relatively low energies. The latter is the case of the muon magnetic anomaly, often referred to as the muon $g-2$ problem. To answer the question, whether some new physic plays a role in this case, one needs to achieve a high precision in both, theoretical prediction and experimental measurement.

The muon gyromagnetic ratio relates the muon spin and magnetic momentum $\overrightarrow{\mu} = g_\mu \left(e/2m_\mu\right) \overrightarrow{s}$ and the magnetic anomaly is defined by $a_\mu = \left(g_\mu - 2\right)/2$. The higher muon mass makes its magnetic momentum, in comparison to the magnetic momentum of the electron, more sensitive to the non-perturbative hadronic effects and thus can the a_μ determination serve as a good test field of the theory of strong interactions. A high-precision experimental result is available, the anomaly a_μ was measured by the $g-2$ collaboration in the E821 experiment at BNL with unprecedent precision of 0.7 ppm [1]. A high-precision theoretical prediction is available also, but only in the electromagnetic and electroweak sector the accuracy is satisfactory. In case of the hadronic contribution a_μ^{had} more precision is desirable, because this contribution is the dominant source of the total uncertainty of the theoretical prediction, which does not allow to conclude on possible physics beyond the SM. Depending on the author and the analyzed data one can cite different numbers. If one takes the values from the summary publication [2] $a_\mu^{exp} = 116\,592\,093\,(63) \times 10^{-11}$ and $a_\mu^{th} = 116\,591\,810\,(210) \times 10^{-11}$ one observes $\triangle a_\mu \approx 1.3\sigma_{\triangle a_\mu}$, $\triangle a_\mu = \left|a_\mu^{th} - a_\mu^{exp}\right|$.

The hadronic part is dominated by the lowest order and this can be calculated using the formula

$$a_\mu^{had,LO} = \frac{1}{3}\left(\frac{\alpha}{\pi}\right)^2 \int_{4m_\pi^2}^{\infty} \frac{ds}{s} K(s) R(s), \tag{1}$$

where $K(s) = \int_0^1 dx[x^2(1-x)]/[x^2 + (1-x)\frac{s}{m_\mu^2}]$ and $R(s) = \sigma_{LO}\left(e^+e^- \to had\right)/\frac{4\pi\alpha^2}{3s}$. The most important contribution comes from the pion channel $a_\mu^{had,LO}(e^+e^- \to \pi^+\pi^-)$, which we study in this work. The data are used to evaluate the integral up to few GeV, above a perturbative calculation is possible. In order to compare to other authors we chose three different limits for the upper integration limit ($3.24\,\mathrm{GeV}^2$, $2.0449\,\mathrm{GeV}^2$ and $0.8\,\mathrm{GeV}^2$).

The expression (1) was up to now [3,4] always evaluated only by the direct integration of the $\sigma_{LO}\left(\pi^+\pi^-\right)$ data (with small exceptions, see [5]).

Our motivation and our aim is to demonstrate, that the use of an appropriate model allows for a dramatic error reduction. The error reduction in this domain is of a crucial importance, since there is an effort to decrease even more the experimental error [6] and so, if one wants to solve the $g-2$ puzzle, the theoretical precision will have to follow.

2. Unitary and Analytic Model of the Pion Electromagnetic Form Factor

We base our evaluation of $a_\mu^{had,LO}(\pi^+\pi^-)$ on the unitary and analytic (U&A) model of the pion electromagnetic (EM) form factor and relate the form factor to the cross section $\sigma_{tot}(e^+e^- \to \pi^+\pi^-) = \frac{\pi\alpha^2}{3t}\left(1-4m_\pi^2/t\right)^{\frac{3}{2}}|F_\pi(t)|^2$, so as to obtain $R(s)$. For a reliable prediction one needs to construct a model that incorporates all known properties of the pion EM form factor. The form factor is charge-normalized $F_\pi(0)=1$ and pQCD predicts its asymptotic behavior $F_\pi(t)_{|t|\to\infty} \sim t^{-1}$, where $t = q^2 = -Q^2$. It is known, that $F_\pi(t)$ is an analytic function in the whole complex t plane, besides the branch points and the cut on the positive real axis, the cut going from the lowest branch point $t_0 = 4m_\pi^2$ up to $+\infty$. The pion form factor has also cut on the second, unphysical Riemann sheet for $-\infty < t < 0$ and satisfies the unitarity condition $Im\left[F_\pi(t)\right] = \left[A_1^1(t)\right]^* F_\pi(t) + \sigma(t)$, where $A_1^1(t)$ is the P-wave isovector transition amplitude for elastic $\pi^+\pi^-$ scattering and $\sigma(t)$ approximates all higher contributions. For $4m_\pi^2 < t < (m_\pi + m_\omega)^2$ one has $\sigma(t) = 0$ and arrives to the so-called elastic unitarity condition.

The construction of the U&A model starts from the Vector Meson Dominance (VMD) picture in which

$$F_\pi(t) = \sum_{v=\rho,\rho',\rho''} \frac{m_v^2}{m_v^2 - t}\left(\frac{f_{v\pi\pi}}{f_v}\right),$$

where $f_{v\pi\pi}$ is the vector meson-pion coupling constant, f_v is the universal vector meson coupling constant and three resonances are taken into account. We proceed to a non-linear transformation

$$t = t_0 - \frac{4(t_{in}-t_0)}{[1/W - W]^2}$$

in order to build in the cut, the lowest branch point t_0 and an effective branch point t_{in}, the latter meant to approximate all higher branch points. The model then becomes

$$F_\pi(W) = \left(\frac{1-W^2}{1-W_N^2}\right)^2 \times \sum_{v=\rho,\rho',\rho''}\left[\frac{(W_N - W_{v0})(W_N + W_{v0})}{(W - W_{v0})(W + W_{v0})} \times \frac{(W_N - 1/W_{v0})(W_N + 1/W_{v0})}{(W - 1/W_{v0})(W + 1/W_{v0})}\left(f_{v\pi\pi}/f_v\right)\right],$$

where $W_N = W(t)|_{t=0}$ and $W_{v0} = W(t)|_{t=m_v^2}$. The expression can be modified further; it can be shown that depending on the relative positions of thresholds and masses one has $t_0 < m_v < t_{in} \Rightarrow W_v = -W_v^*$ and $t_{in} < m_v \Rightarrow W_v = 1/W_v^*$. The masses and t_{in} are considered as free parameters of the model and so their relative positions are not fixed. However, in order to provide explicit formulas in the following text, we will here suppose $t_0 < m_\rho < t_{in} < m_{\rho'}, m_{\rho''}$, what is actually being confirmed by the result of the data fitting.

The next step in the model construction is incorporation of the cut on the second Riemann sheet. We use a succession of poles and zeros generated by a rational function to approximate this cut (Padé approximation). We do it by adding to the model a multiplicative term $\frac{(W-W_Z)(W_N-W_P)}{(W_N-W_Z)(W-W_P)}$, where W_Z and W_P are free parameters from the interval $0 < W_{Z,P} < 1$ (corresponds to $-\infty < t < 0$). The construction of the model is finally achieved by giving the vector mesons non-zero decay widths $W_{v0} \to W_v = W(t)|_{t=\left(m_v - i\frac{\Gamma_v}{2}\right)^2}$. The model gets form

$$F_\pi[W(t)] = \left(\frac{1-W^2}{1-W_N^2}\right)^2 \frac{(W-W_Z)(W_N-W_P)}{(W_N-W_Z)(W-W_P)} \times \left[\frac{(W_N - W_\rho)\left(W_N - W_\rho^*\right)}{(W - W_\rho)\left(W - W_\rho^*\right)} \times \frac{(W_N - 1/W_\rho)\left(W_N - 1/W_\rho^*\right)}{(W - 1/W_\rho)\left(W - 1/W_\rho^*\right)}\left(f_{\rho\pi\pi}/f_\rho\right) + \sum_{v=\rho',\rho''}\frac{(W_N - W_v)(W_N - W_v^*)}{(W - W_v)(W - W_v^*)}\right.$$

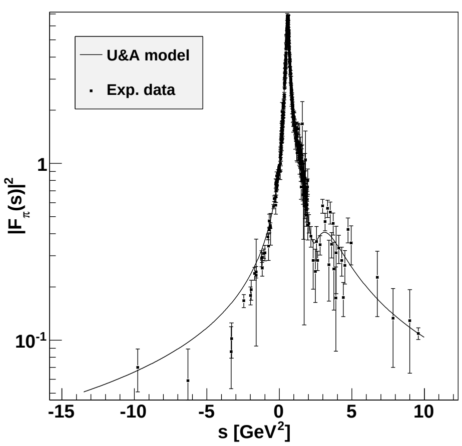

Figure 1. Fit of the data with the U&A model.

$$\times \frac{(W_N + W_v)(W_N + W_v^*)}{(W + W_v)(W + W_v^*)} (f_{v\pi\pi}/f_v) \Big] .$$

The ratio of couplings $f_{\rho\pi\pi}/f_\rho$ is a free parameter of the model, the two remaining ratios, $f_{\rho'\pi\pi}/f_\rho$ and $f_{\rho''\pi\pi}/f_{\rho''}$, can be related to the first one by using the normalization condition $F_\pi(0) = 1$ and by considering the behavior of the imaginary part of the form factor at $q = 0$. The $\rho - \omega$ interference is taken into account when fitting the experimental data by a Breit-Wigner term, the fitting function is

$$F_\pi [W(t)] + Re^{i\phi} \frac{m_\omega^2}{m_\omega^2 - t - im_\omega \Gamma_\omega},$$

where $\phi = \arctan \frac{m_\rho \Gamma_\rho}{m_\rho^2 - m_\omega^2}$ and the amplitude R is considered as an additional free parameter. The fitting function thus has 11 free parameters in total (t_{in}, three masses, three widths, ratio $f_{\rho\pi\pi}/f_\rho$, W_z, W_P and R) and is used to fit 523 experimental points measured in experiments *CLEO*, *NA7*, *OLYA*, *CMD*, *CMD-2*, *SND*, *KLOE*, in *JINR* Dubna and in F_π collaboration at Jefferson Lab [7,8,9,10,11,12,13,14,15,16,17,18,19,20,21,22, 23,24,25,26,27,28,29,30,31,32,33,34]. The best fit result is shown in Figure 1.

3. Error Evaluation and Results

Two approaches were used for the error evaluation. The first one was a "Monte Carlo" method based on a random number generator with the assumption of the Gaussian distribution for the uncertainties of the published data points. For each point a new one was randomly generated using the Gaussian probability density function with the mean identical to the original point and σ equal to the published error. Doing this for each point, new "random" data set was obtained. This data set was then fitted and the values of the parameters of the model p_i as well as the value of $a_\mu^{had,LO}(\pi^+\pi^-)$ were extracted. Repeating the whole procedure 4000 times, we reached statistics high enough to allow us for a reliable error calculation. The mean $\overline{a_\mu^{had,LO}}(\pi^+\pi^-)$ and the σ were calculated from the 4000 values and since the mean is not, in general, identical with the optimal-fit value $a_{\mu,OPT}^{had,LO}(\pi^+\pi^-)$ we present asymmetric uncertainties $a_\mu^{had,LO}(\pi^+\pi^-) = a_{\mu,OPT}^{had,LO}(\pi^+\pi^-)^{-A}_{+B}$, where $A = \sigma + a_{\mu,OPT}^{had,LO}(\pi^+\pi^-) - \overline{a_\mu^{had,LO}}(\pi^+\pi^-)$ and $B = \sigma + \overline{a_\mu^{had,LO}}(\pi^+\pi^-) - a_{\mu,OPT}^{had,LO}(\pi^+\pi^-)$.

In the second approach the program MINUIT was used to establish the uncertainties of the model parameters. Then, taking the numerical derivatives for $\frac{\partial}{\partial p_i} a_\mu^{had,LO}(\pi^+\pi^-)$, the uncertainty was propagated to $a_\mu^{had,LO}(\pi^+\pi^-)$ using the covariance matrix. In this method the errors are symmetric.

In addition to the integration of the model, we also performed a direct integration of the data points based on the trapezoidal rule, so as to cross-check our compatibility with other authors. Our results and some results from other authors [3,4,5] are summarized in Table 1.

4. Discussion, Summary and Outlook

The use of the U&A model dramatically reduces the error on $a_\mu^{had,LO}(\pi^+\pi^-)$. This is not an arbitrary feature of the model but originates from model-independent information which is additional to the data in the integration region and which can be taken into account when the model

	$a_\mu^{had,LO}(e^+e^- \to \pi^+\pi^-) \times 10^{11}$		
Interval $[GeV^2]$	$4m_\pi^2 < t < 3.24$	$4m_\pi^2 < t < 2.0449$	$4m_\pi^2 < t < 0.8$
Model, method 1	$5132.36^{-0.83}_{+0.83}$	$5128.22^{-0.67}_{+0.73}$	$4870.24^{-0.20}_{+0.20}$
Model, method 2	5132.37 ± 3.00	5128.25 ± 2.86	4870.44 ± 2.64
Data	$5035.33^{-17.22}_{+28.32}$	$5031.22^{-16.43}_{+28.94}$	$4756.77^{-18.14}_{+27.55}$
Davier	5040.00 ± 31.05		
Hagiwara et al.		5008.2 ± 28.70	
Ynduráin et al.			4715 ± 33.53

Table 1
Our results and results of other authors [3,4,5].

is used. The most important sources contributing to error reduction are

- Expected smoothness of the $F_\pi(t)$ at small scale Δt: The model provides a function behaving smoothly at small Δt.

- Experimental data outside the integration region: The fit is done not only to the data inside, but also to the data outside the integration region.

- Theoretical knowledge on $F_\pi(t)$: The model respects all known properties of the pion EM form factor.

Especially the first point plays an important role. The new precise data tend to lie above older, less precise data and, in some regions, the vertical spread of the data is very important, at the limit of inconsistency. If the calculation of the integral is based directly on data, then less precise data shift the mean value of the integral and enlarge the uncertainty. When the model is used, the predicted behavior of $F_\pi(t)$ as given by the result of the fit is mostly determined by precisely measured points and is only little influenced by data with important uncertainties. This leads to more appropriate mean value and smaller errors. In consequence, one arrives to the mean value of $a_\mu^{had,LO}(\pi^+\pi^-)$ which is higher then what is obtained by the direct data integration and to much reduced uncertainty. The shift in the mean value goes in the "right" direction and brings the theoretical value closer to the experimental one.

The error estimates from the two used methods are not fully compatible, the first method gives smaller errors. This might be related to statistical fluctuations (1st method) and to approximations - numerical derivatives and linearization (2nd method).

In this article we presented the calculation of $a_\mu^{had,LO}(\pi^+\pi^-)$ based on the U&A model. This approach allows for important error reduction and we plan to use it also for evaluating the contributions of other channels to $a_\mu^{had,LO}$.

Acknowledgments

The work was partly supported by Slovak Grant Agency for Sciences VEGA, grant No. 2/7116/29.

REFERENCES

1. G. W. Bennett, et al., Phys. Rev. D 73 (2006).
2. P. J. Mohr, B. N. Taylor, and D. B. Newell, Rev. Mod. Phys 80(2), 633-730(2008).
3. M. Davier, Nucl. Phys. B Proc. Supp. 169 (2007) 288.
4. K. Hagiwara, A. D. Martin, D. Nomura and T. Teubner, Phys. Lett. B649 (2007) 173.
5. J. F. de Trocóniz and F. J. Ynduráin, Phys. Rev. D71 (2005) 073008.
6. D. W. Hertzog, Nucl. Phys. Proc. Suppl. 169 (2007) 255.
7. C. J. Bebek et al., Phys. Rev. D17 (1978) 1693.
8. P. Brauel et al., Phys. Lett. 69B (1977) 253.

9. S. R. Amendolia et al., Nucl. Phys. B277 (1986) 168.
10. E. B. Dally et al., Phys. Rev. Lett. 48 (1982) 375.
11. S. F. Berezhnev et al., Yad. Fizika 24 (1976) 1127.
12. S. F. Berezhnev et al., Yad. Fizika 18 (1973) 102.
13. S. F. Berezhnev et al., Yad. Fizika 16 (1972) 185.
14. S. R. Amendolia et al., Phys. Lett. 138B (1984) 454.
15. L. M. Barkov et al., Nucl. Phys. B256 (1985) 365.
16. I. B. Vassermanet et al., Yad. Fizika 33 (1982) 709.
17. A. Quenzer et al., Phys. Lett. 76B (1978) 512.
18. A. Quenzer et al., Preprint LAL-1282, ORSAY (1975).
19. D. Benaksas et al., Phys. Lett. 39B (1972) 289.
20. A. D. Bukin et al., Phys. Lett. 73B (1978) 226.
21. G. Cosme et al., Preprint LAL-1287, ORSAY (1976).
22. V. B. Balakin et al., Phys. Lett. 34B (1971) 28, ibid 41B (1972) 205.
23. D. Bollini et al., Nuovo Cimento Lett. 14 (1975) 418.
24. B. Esposito et al., Nuovo Cimento Lett. 28 (1980) 337.
25. D. Bisello et al., Phys. Lett. 220B (1989) 321.
26. R. M. Baltrusaitis et al., Phys. Rev. D32 (1985) 566.
27. Akhmetshin et al., Physics Letters B 578 (2004) 285-289.
28. Auľchenko et al., JETP Letters, Vol. 82, No. 12 (2005) 743-747.
29. Auľchenko et al., JETP Letters, 2006, Vol. 84, No. 8, 413-417.
30. Akhmetshin et al., Physics Letters B 648 (2007) 28-38.
31. Achasov et al., JETP, 2006, Vol. 103, No. 3, 380-384.
32. Aloisio et al., Physics Letters B 606 (2005) 12-24.
33. T. Pedlar et al. (CLEO Collaboration), Phys. Rev. Lett. 95, 261803 (2005).
34. Huber et al., Physical Review C 78, 045203 (2008).